Tetranuclear iron(III) complexes of an octadentate pyridine-carboxylate ligand and their catalytic activity in alkane oxidation by hydrogen peroxide†

Elena A. Gutkina,[a] Vladimir M. Trukhan,[a,b] Cortlandt G. Pierpont,*[c] Shaen Mkoyan,[a] Vladimir V. Strelets,[a] Ebbe Nordlander*[b] and Albert A. Shteinman*[a]

Received 25th August 2005, Accepted 2nd September 2005
First published as an Advance Article on the web 10th October 2005
DOI: 10.1039/b512069a

Reaction of the octadentate ligand 2,6-bis{3-[*N*,*N*-di(2-pyridylmethyl)amino]propoxy}benzoic acid (LH) with $Fe(ClO_4)_3$ leads to the formation of the tetranuclear complexes $[Fe_4(\mu\text{-}O)_2(LH)_2(ClCH_2\text{-}CO_2)_4](ClO_4)_4$ (**1**), $[\{Fe_2(\mu\text{-}O)L(R\text{-}CO_2)\}_2](ClO_4)_4$ (**2** R = C_6H_5-, **3** R = CH_3-, **4**, R = $ClCH_2$-). The crystal structures of complexes **1** and **2** reveal that they consist of two $Fe^{III}_2(\mu\text{-}O)(\mu\text{-}RCO_2)_2$ cores that are linked *via* the two LH/L ligands to give a "dimer of dimers" structure. Complex **1** assumes a helical shape, with protonated carboxylic acid moieties of the two ligands forming a hydrogen-bonded pair at the center of the cation. In complexes **2**, **3** and **4**, central carboxylates of the two ligands bridge the iron ions in each of the two Fe_2O units, with an interdimer iron–iron separation of approximately 10 Å and an intradimer separation of approximately 3.1 Å. The second carboxylate bridge within the Fe_2O units is defined by exogenous benzoate (**2**), acetate (**3**) or chloroacetate (**4**) ligands. The aqua complex $[\{Fe_2(\mu\text{-}O)L(H_2O)_2\}_2](ClO_4)_6$ (**5**) is proposed to have a similar structure, but with the exogenous bridging carboxylates replaced by two terminal water ligands. These complexes exhibit electronic and Mössbauer spectral features that are similar to those of (μ-oxo)diiron(III) proteins as well as other related (μ-oxo)bis(μ-carboxylato)diiron(III) complexes. This similarity shows that these properties are not significantly affected by the nature of the bridging exogenous carboxylate, and that the octadentate framework ligand is essential in stabilizing the "dimer of dimers" structure. This structural feature remains in highly diluted solution (10^{-5} M) as evidenced by electrospray ionization mass-spectroscopy (ES MS). Cyclic voltammetric studies of complexes **2** and **5** showed two irreversible two-electron reductions, indicating that the two Fe_2O units of the tetranuclear complexes behave as distinct redox entities. Complexes **2**, **3** and, especially, the aqua complex **5** are active alkane oxidation catalysts. Catalytic reactions carried out with alkane substrate molecules and hydrogen peroxide predominantly gave alcohols. High stereospecificity in the oxidation of *cis*-1,2-dimethylcyclohexane supports the metal-based molecular mechanism of O-insertion into C–H bonds postulated for non-heme iron enzymes such as methane monooxygenase.

Introduction

A number of Fe_2O complexes has been synthesized to model the spectroscopic and structural properties of μ-oxo-μ-carboxylato diiron sites in proteins such as soluble methane monooxygenase (sMMO), ribonucleotide reductase (RNR) and hemerythrin.[1] In many cases, such biomimetic complexes have been found to be relatively unstable.[1,2] Efforts have therefore been made to prepare framework polydentate ligands that may stabilize complexes of this type.[3] Examples include ligands in which multidentate nitrogen-donors that bind to metals in a capping manner are linked to alkoxo or phenoxo groups capable of bridging two metals.[4] Binucleating polydentate ligands containing nitrogen donors linked to a carboxylate moiety should be even more relevant for modeling μ-oxo-μ-carboxylate diiron sites since the carboxylate bridges in these enzymes are part of the protein.[5,6] Two successful[7,8] and two unsuccessful[9,10] attempts have been reported for the preparation of dinuclear iron complexes containing similar ligands; in these ligands, the carboxylate is one of the "peripheral" donors at the terminus of a polydentate ligand. Successful structural and functional modeling of sMMO constitutes a special challenge, requiring the preparation of diiron complexes that not only model structural features of the sMMO active site but that are also capable of effecting alkane oxidation by a metal based mechanism involving peroxide and high valent iron oxo intermediates.[1a,11] The significant criteria of this mechanism are stereospecific alkane oxidation[12] and incorporation of ^{18}O from $H_2{}^{18}O$ in product alcohol.[13]

We recently described the synthesis of the ligand 2,6-bis{3-[*N*,*N*-di(2-pyridylmethyl)amino]propoxy}benzoic acid (LH), containing a potentially bridging carboxylate moiety included as part of a spacer that links two di(picolyl)amine groups, as well as the synthesis and structure determination of the tetranuclear iron(III) complex $[Fe_4(\mu\text{-}O)_2(LH)_2(ClCH_2CO_2)_4](ClO_4)_4$ (**1**).[14] Complex **1**, containing two distinct (μ-oxo)bis(μ-chloroacetato)diiron(III)

[a]*Institute of Problems of Chemical Physics, 142432, Chernogolovka, Moscow district, Russia. E-mail: ast@icp.ac.ru*
[b]*Inorganic Chemistry, Chemical Center, Lund University, Box 124, SE-221 00, Lund, Sweden. E-mail: Ebbe.Nordlander@inorg.lu.se*
[c]*Department of Chemistry and Biochemistry, University of Colorado, Boulder, CO, 80309-0215, USA. E-mail: Pierpont@Colorado.edu*

† Electronic supplementary information (ESI) available: NMR spectra of complexes **2**, **3** and **5**. See DOI: 10.1039/b512069a

cores, was shown to have a helical shape formed by bridging LH ligands joined by hydrogen-bonded carboxylic acid moieties (Fig. 1). We have since found that different reaction conditions permit the isolation of tetranuclear iron complexes in which the carboxylate of L bridges adjacent diiron cores. Here, we report the synthesis and characterization of a series of complexes, $[\{Fe_2(\mu\text{-}O)L(R\text{-}CO_2)\}_2](ClO_4)_4$ (R = Ph **2**, CH_3 **3**, CH_2Cl **4**), in which the two iron ions in each Fe_2O unit are coordinated by the carboxylate of L as well as an exogenous carboxylate anion. In addition, we present the syntheses and characterization of the related aquo complex $[\{Fe_2(\mu\text{-}O)L(H_2O)_2\}_2](ClO_4)_6$ **5**. Comparative studies of ^{1}H-NMR, Mössbauer spectra and the electrochemical behavior of complexes **1–5** are described, as well as the results of an investigation into their activity as alkane oxidation catalysts.

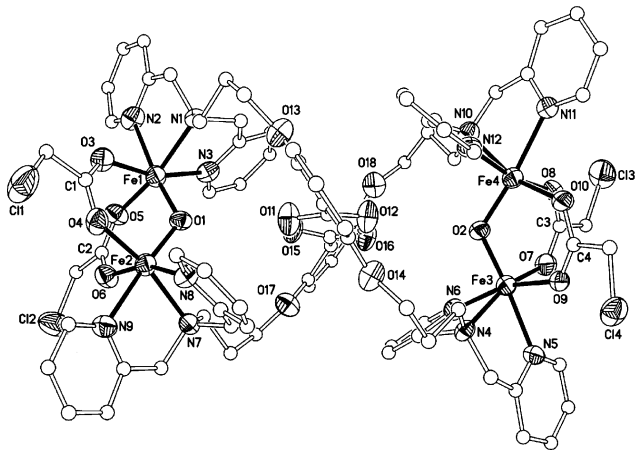

Fig. 1 An ORTEP drawing of the molecular structure of the $[Fe_4O_2(LH)_2(\mu\text{-}O_2CCH_2Cl)_4]^{4+}$ cation **1**[14] showing the atom labeling scheme. Thermal ellipsoids are drawn at the 30% level.

Experimental

General considerations

All reagents and solvents were of commercial reagent grade and were used without further purification except where noted. Dry methanol was obtained by distillation over CaH_2. Solvents used for spectroscopic measurements were all spectroscopic grade. Preparative separations were performed by silica gel flash column chromatography (Merck Kieselgel 6). *N*,*N*-bis(2-pyridylmethyl)amine (dipicolylamine) was synthesized in 78% yield according to a literature procedure.[15]

Physical methods

^{1}H NMR spectra were recorded in $CDCl_3$ or acetonitrile-d_3 solutions on a Varian UNITY 300 MHz spectrometer; chemical shifts are given as values in ppm relative to the solvent resonances. Electrospray mass spectra in CH_3CN were recorded on a prototype of a time-of flight mass spectrometer equipped with an ion source with ES ionization. The instrument and its principle of operation have been described in detail.[16] UV-visible spectra (200 to 900 nm) were recorded on a Milton Roy 3000 spectrophotometer. Electrochemical measurements were performed in acetonitrile solution using a PAR 173 potentiostat with a PAR 175 signal generator. The cyclic voltammetry studies were carried out over a potential range of +1 to −2 V (*vs.* SCE) using a scan rate of 0.2 V s^{-1} at 15 °C.

Methyl 2,6-di(3-bromopropoxy)benzoate

Powdered K_2CO_3 (26.5 g 184 mmol) and 1,3-dibromopropane (50 ml, 247 mmol) were added to a solution of methyl resorcylate (8 g, 47.6 mmol) in dry acetone (500 ml). The mixture was refluxed for 3 days under N_2. Then the solution was filtered, and the acetone solution containing an excess of 1,3-dibromopropane was evaporated under reduced pressure. The remaining residue was redissolved in benzene and chromatographed on a silica-gel column (230–400 mesh, elution with benzene) to yield 19.0 g (94.4%) of colorless crystals of methyl 2,6-di(3-bromopropoxy)benzoate with mp 34–38 °C. Anal. Calcd for $C_{14}H_{18}Br_2O_4$, (%): C, 41.00; H, 4.42; Br, 38.97. Found (%): C, 41.32; H, 4.45; Br, 38.90. ^{1}H NMR (300 MHz, $CDCl_3$, ppm): 7.26 t, (1 H, C_6H_3); 6.57 d, (2 H, C_6H_3); 4.13 t, (4 H, Br–CH_2); 3.87 s, (3 H, $COOCH_3$); 3.54 t, (4 H, O–CH_2); 2.27 p, (4 H, CH_2).

Methyl 2,6-di(3-(di(2-pyridylmethyl)amino)propoxybenzoate (LMe)

Dipicolylamine (1.467 g, 7.38 mmol), triethylamine (1.12 g, 11.06 mmol) and methyl 2,6-di(3-bromopropoxy)benzoate (1.5 g, 3.65 mmol) were dissolved in absolute THF (50 ml). The solution was refluxed for four days under a nitrogen atmosphere. Then the solid material was filtered off and the solvent was removed by vacuum evaporation. The residue was dissolved in 200 ml of diethyl ether, washed three times with 100 ml portions of water, and dried over $MgSO_4$. After evaporation, the residue was chromatographed on a silica-gel column (230–400 mesh, elution with ethyl acetate–methanol, 9 : 1) to yield a product with R_f 0.57 in methanol. Yellow oil, 1.81 g (76.7%). Anal. Calcd for $C_{38}H_{42}N_6O_4$, (%): C, 70.59; H, 6.50; N, 13.00 Found (%): C, 70.56; H, 6.55; N, 13.00. ^{1}H NMR (300 MHz, $CDCl_3$, ppm): 8.5 d, (4 H, CH=N); 7.58 t, (4 H, C_5H_4N); 7.46 d, (4 H, C_5H_4N); 7.18 t, (1 H, C_6H_3); 7.10 t, (4 H, C_5H_4N); 6.45 d, (2 H, C_6H_3); 3.97 t, (4 H, O–CH_2); 3.82 s, (8 H, N–CH_2–C_5H_4N); 3.61 s, (3 H, $COOCH_3$); 2.7 t, (4 H, N–CH_2); 1.96 t, (4 H, CH_2).

2,6-Di(3-(di(2-pyridylmethyl)amino)propoxybenzoic acid (LH)

The methyl ester LMe (1 g, 1.54 mmol) was dissolved in 50 ml of a 5% ethanol solution of KOH and refluxed gently for 36 h. After the solvent was evaporated, the residue was dissolved in 10 ml of water, acidified with concentrated hydrochloric acid to pH 7 and extracted with ethyl acetate. The combined ethyl acetate solution was then dried over $MgSO_4$ and the solvent was removed under reduced pressure to give 840 mg (86.6%) of an amorphous yellow solid. Anal. Calcd for $C_{37}H_{40}N_6O_4$, %: C, 70.23; H, 6.37; N, 13.28. Found%: C, 70.57; H, 6.54; N, 12.99. ^{1}H NMR (300 MHz, $CDCl_3$, ppm): 8.4 d, (4 H, CH=N); 7.55 t, (4 H, C_5H_4N); 7.38 d, (4 H, C_5H_4N); 7.18 t, (1 H, C_6H_3); 7.05 t, (4 H, C_5H_4N); 6.51 d, (2 H, C_6H_3); 4.02 t, (4 H, O–CH_2); 3.85 s, (8 H, N–CH_2–C_5H_4N); 2.85 t, (4 H, N–CH_2); 1.96 t, (4 H, CH_2).

$[Fe_4O_2(LH)_2(\mu\text{-}O_2CCH_2Cl)_4](ClO_4)_4$ (1). Chloroacetic acid (200 mg, 2.128 mmol) was dissolved in 5 ml of acetonitrile and

the mixture was added dropwise to a solution of $Fe(ClO_4)_3{\cdot}9H_2O$ (160 mg, 0.31 mmol) in 3 ml of acetonitrile. To this solution, the acid LH (98 mg, 0.155 mmol) in 2 ml of methanol was added. Brown crystals of **1** precipitated within two days giving 120 mg of the complex in 65% yield as an unstable mixed water/methanol solvate. UV-Vis [MeCN; λ_{max}/nm (ε_M(Fe)/M^{-1} cm^{-1}): 211 (23 000), 245 sh (15 000), 344 (4200), 380 sh (3100), 472 (840), 510 (730), 555 sh (220), 721 (155). IR (KBr), ν/cm^{-1}: 1687 (CO_2H), 1607 (Py), 1570 ($\nu_{as}COO^-$), 1463, 1418 ($\nu_s COO^-$), 536 (ν_sFe–O–Fe). ^{1}H NMR (CD_3CN, 25 °C): 28 (o-*H*(Py)), 15.6 (Py–CH_2–N), 12.0 (*m*-*H*(Py)), 11.5 (O_2CCH_2Cl), 8.5 (*m*-(*H*)Ph), 7.8 (*p*-(*H*)Ph), 7.4 (*p*-(*H*)Py), 6.7, 5.4, 4.1 (CH_2); ESMS—see text.

[{Fe$_2$(μ-O)(L)(μ-O$_2$CC$_6$H$_5$)}$_2$](ClO$_4$)$_4$ (2). Sodium benzoate (45.5 mg, 0.316 mmol) in 2 ml of methanol was added to an acetonitrile solution containing $Fe(ClO_4)_3{\cdot}9H_2O$ (163 mg, 0.316 mmol) whereupon the mixture turned pale brown/green. Then the acid LH (100 mg, 0.158 mmol) in 5 ml of acetonitrile was added to the solution and the mixture turned deep green/brown. The solution was left for several days as brown crystals of complex **2** formed. The complex was obtained in 44.7% yield (80 mg) as an unstable mixed water/acetonitrile solvate. UV-Vis [MeCN; λ_{max}/nm (ε_M(Fe)/M^{-1} cm^{-1}): 235 (78 000), 340 (17 600), 470 (2700), 505 (2100), 550 sh (750), 725 (450). IR (KBr), ν/cm^{-1}: 3420; 1607; 1539 ($\nu_{as}COO^-$); 1463; 1405 ($\nu_s COO^-$); 1265; 1088 (ClO_4^-); 763; 715; 625 (ClO_4^-); 539 (ν_sFe–O–Fe); 475; 418. ^{1}H NMR (CD_3CN, 25 °C): 28.4 (*o*-*H*(Py)), 15.49 (N–CH_2–Py), 12.14 (*m*-*H*(Py)), 11.62 (*m*-*H*(Py)), 8,5 (*m*-*H*(Ph)), 7.9 (*p*-*H*(Ph)), 7.7 (*p*-*H*(Py)), 6.83, 6.28, 5.45, 3.95 (CH_2); ESMS (*m*/*z*, amu) 979(M^+), 619 ({[$Fe_2OL(OBz)]_2(ClO_4)$}$^{3+}$), 440 ([$Fe_2OL(OBz)]_2^{4+}$).

[{Fe$_2$(μ-O)(L)(μ-O$_2$CCH$_3$)}$_2$](ClO$_4$)$_4$ (3). Sodium acetate (26 mg, 0.316 mmol) in 2 ml of methanol was added to an acetonitrile solution containing $Fe(ClO_4)_3{\cdot}9H_2O$ (163 mg, 0.316 mmol), whereupon the mixture turned pale brown/green. The acid LH (100 mg, 0.158 mmol) in 2 ml of acetonitrile was added to the solution and the mixture turned deep green/brown. Slow evaporation gave brown crystals of complex **3** in 55.4% yield (98 mg) as a water/methanol solvate, [{Fe_2(μ-O)(L)(μ-O_2CCH_3)}$_2$](ClO$_4$)$_4{\cdot}6H_2O{\cdot}2CH_3OH$. Anal. Calcd for $C_{80}H_{104}Cl_4Fe_4N_{12}O_{40}$, %: C, 43.54; H, 4.75; Cl, 6.43; Fe, 10.12; N, 7.62. Found%: C, 43.3; H, 4.1; Cl, 6.3; N, 7.7. UV-Vis [MeCN; λ_{max}/nm (ε_M(Fe)/M^{-1} cm^{-1}): 212 (60 000), 255 sh, 344 (12 400), 467 (2650), 505 (2200), 550 sh (800), 723 (700). IR (KBr), ν/cm^{-1}: 3422; 1607; 1547 ($\nu_{as}COO^-$); 1463; 1439 ($\nu_s COO^-$); 1265; 1090 (ClO_4^-); 768; 625 (ClO_4^-); 535 (ν_sFe–O–Fe); 473. ^{1}H NMR (CD_3CN, 25 °C): 27.5 (*o*-*H*(Py)), 15.47 (N–CH_2–Py), 12.06 (*m*-*H*(Py)), 11.56 ($COOCH_3$), 8,49 (*m*-*H*(Ph)), 7.34 (*p*-*H*(Ph)), 6.73, 6.3, 5.45, 3.9 (CH_2); ESMS (*m*/*z*, amu) 917 (M^+), 578 ({[$Fe_2OL(OAc)]_2(ClO_4)$}$^{3+}$), 409 {[$Fe_2OL(OAc)]_2(ClO_4)_2$}$^{2+}$.

[{Fe$_2$(μ-O)(L)(μ-O$_2$CCH$_2$Cl)}$_2$](ClO$_4$)$_4$ (4). Chloroacetic acid (29.74 mg, 0.316 mmol) in 5 ml of acetonitrile was added to an acetonitrile solution containing $Fe(ClO_4)_3{\cdot}9H_2O$ (163 mg, 0.316 mmol). The mixture turned green. The acid LH (100 mg, 0.158 mmol) in 2 ml of acetonitrile was added to the green solution and the mixture turned green/brown. The solution was left overnight to precipitate brown crystals of complex **4** as a water/methanol solvate. Yield 103 mg (58.2%). Anal. Calcd for $C_{80}H_{98}Cl_6Fe_4N_{12}O_{36}$, %: C, 42.90; H, 4.41; Cl, 9.50; Fe, 9.97; N, 7.50; Found%: C, 42.3; H, 3.95; Cl, 9.4; N, 7.6. UV-Vis [MeCN; λ_{max}/nm (ε_M(Fe)/M^{-1} cm^{-1}): 210 (80 500), 241 (61 700), 344 (19 100), 472 (3200), 510 (2647), 550 sh (800), 725 (470). IR (KBr), ν/cm^{-1}: 3417; 1608; 1579 ($\nu_{as}COO^-$); 1463; 1416 ($\nu_s COO^-$); 1265; 1088 (ClO_4^-); 767; 625 (ClO_4^-); 530 (ν_sFe–O–Fe); 415. ^{1}H NMR (CD_3CN, 25 °C): 29 (*o*-*H*(Py)), 15.68 (N–CH_2–Py), 12.0 (*m*-*H*(Py)), 11.6 ($COOCH_2Cl$), 8,5 (*m*-*H*(Ph)), 7.76 (*p*-*H*(Ph)), 6.7, 5.44, 4.1 (CH_2); ESMS—see text.

[{Fe$_2$O(L)(H$_2$O)$_2$}$_2$](ClO$_4$)$_6$ (5). The acid LH (50 mg, 0.08 mmol), dissolved in 3 ml of ethanol was mixed with $Fe(ClO_4)_3{\cdot}9H_2O$ (83 mg, 0.16 mmol) dissolved in 2 ml of ethanol. A brown/green powder precipitated. The complex was isolated by filtration and washed with ethanol. It was obtained as an unstable hydrate in 71.7% yield (62 mg). UV-Vis [MeCN; λ_{max}/nm (ε_M(Fe) M^{-1} cm^{-1})]: 220 (35 000), 259 (20 000), 330 (4000), 474 (659), 520 sh (535), 724 (97). IR (KBr), ν/cm^{-1}:1608, 1541 ($\nu_{as}COO^-$), 1463, 1419 ($\nu_s COO^-$), 537 (ν_sFe–O–Fe), 473. ^{1}H NMR (CD_3CN, 25 °C): δ 26 (*o*-py), 15.4, 14.0 (pyCH_2N), 11.6, 11.3 (*m*-py), 8.9, 8.6 (*m*-Ph), 8.0 (*p*-Ph), 7.3 (*p*-Py), 6.7, 4.4, 3.9, 3.6 (CH_2). *Cf.* ref. 14 for microanalytical data.

Crystallographic studies

Crystals of **1** and **2** suitable for X-ray diffraction studies were grown by slow evaporation of acetonitrile/methanol solutions. Crystals of both complexes were observed to lose solvent within seconds upon separation from the recrystallization solution. Crystallographic data are summarized in Table 1.

[Fe$_4$O$_2$(LH)$_2$(μ-O$_2$CCH$_2$Cl)$_4$](ClO$_4$)$_4$ (1). A crystal of **1** was mounted on a glass fiber and coated with an amorphous resin to retard crystal deterioration. Data were collected with a Siemens SMART CCD area detector, using graphite-monochromated Mo-Kα radiation ($\lambda = 0.71069$ Å) from a Rigaku rotating anode X-ray generator. Intensity data were corrected for Lorentz, polarization and absorption effects. The positions of the iron atoms were determined using direct methods, and all the non-hydrogen atoms were located from difference Fourier syntheses. The hydrogen

Table 1 Crystallographic data for [{$Fe_2O(LH)(ClCH_2CO_2)_2$}$_2$](ClO$_4$)$_4{\cdot}2$ $CH_3OH{\cdot}H_2O$ (**1**) and [{$Fe_2O(L)(C_6H_5CO_2)$}$_2$](ClO$_4$)$_4$ 2 CH_3CN 2 H_2O (**2**)

	(**1**)	(**2**)
Formula	$Fe_4Cl_8O_{37}N_{12}C_{84}H_{98}$	$Fe_4Cl_4O_{32}N_{14}C_{92}H_{92}$
FW	2372.6	2271.0
Crystal system	Triclinic	Triclinic
Space group	*P*-1	*P*-1
Z	2	1
a/Å	16.4575(3)	13.685(3)
b/Å	17.8346(2)	14.468(3)
c/Å	19.3790(3)	15.670(3)
α/°	77.521(1)	72.65(3)
β/°	89.245(1)	68.65(3)
γ/°	86.432(1)	64.34(3)
V/Å^3	5542.9(2)	2567.9(9)
T/K	293(2)	293(2)
d/g cm^{-3}	1.410	1.494
μ/mm^{-1}	0.788	0.746
R, R_w[a]	0.097, 0.205	0.098, 0.202
GOF	0.854	0.773

[a] Discrepancy indices are defined as: $R = \Sigma\|F_o| - |F|/\Sigma|F_o|$ and $R_w = [\Sigma w(|F_o| - |F_c|)^2/\Sigma w(F_o)^2]^{1/2}$.

atoms were placed in calculated positions. Rotational disorder in the orientations of the CH_2Cl groups of two chloroacetates was detected and successfully modeled using fractional occupancy factors; the conformations shown in Figs. 1 and 2 are for chloride locations with highest occupancy. The final refinement was carried out by full-matrix least-squares calculations on F^2 and with anisotropic thermal parameters for all non-hydrogen atoms.

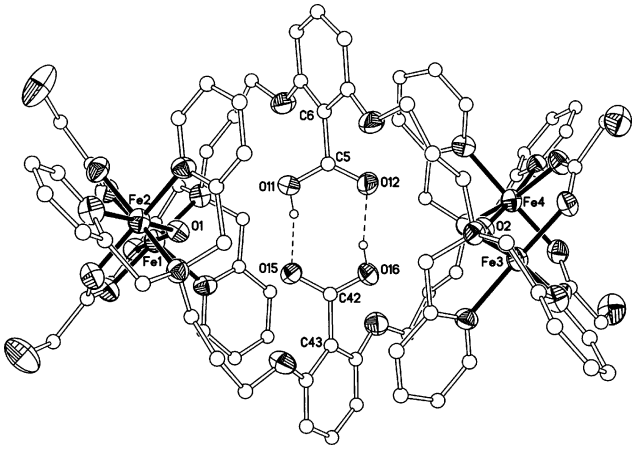

Fig. 2 An ORTEP plot of the $[Fe_4O_2(LH)_2(\mu\text{-}O_2CCH_2Cl)_4]^{4+}$ cation **1** showing the hydrogen bonded carboxylic acid moieties of LH at the center of the dimer.

$[\{Fe_2(\mu\text{-}O)(L)(\mu\text{-}O_2CC_6H_5)\}_2](ClO_4)_4$ (2). A crystal of **2** was placed in a glass capillary with a drop of mother liquor for data collection. Data were collected as before with a Siemens SMART CCD area detector, using graphite-monochromated Mo-Kα radiation ($\lambda = 0.71069$ Å) from a Rigaku rotating anode X-ray generator. Intensity data were corrected for Lorentz, polarization and absorption effects. The locations of the iron atoms and many of the atoms from within the inner coordination sphere were determined from a sharpened Patterson map. The "dimer of dimers" was found to be located about a crystallographic center of inversion symmetry in the triclinic space group *P*-1 (no. 2). After atoms of the cation and perchlorate anions were located, the atoms of water and acetonitrile solvent molecules appeared in the difference Fourier and were included in the refinement.

CCDC reference numbers 127873 (**1**)[14] and 255394 (**2**).

See http://dx.doi.org/10.1039/b512069a for crystallographic data in CIF or other electronic format.

Investigation of catalytic alkane oxidation reactions catalyzed by complexes 2, 3 and 5

Experiments were carried out at 20 °C in glass vials (10 ml) closed by rubber septa. Solutions of alkane and catalyst in MeCN were placed in a vial and the reaction was initiated by addition of hydrogen peroxide with vigorous stirring. The volume of the catalytic solution was approximately 3 ml. Addition of a 30% aqueous solution of H_2O_2 was carried out in two different ways: as a single portion together with other reagents at the beginning of the reaction ("one-pot" experiment) or by slow addition during reaction through a polyethylene capillary tube. The tube was inserted into the catalytic solution through a septum cap and connected to a glass syringe filled with H_2O_2 solution. The rate of addition was controlled by a Cambridge syringe. The solution was stirred for an additional 5 min after H_2O_2 addition was complete. The concentration of catalyst was typically 0.7 0 mM and the H_2O_2 and alkane concentrations were adjusted by addition of MeCN to give a catalyst : peroxide : alkane ratio of 1 : 420 : 1000. The iron complex was removed by passing the solution through a silica gel column followed by elution with 3 ml of MeCN. An internal standard (chlorobenzene) was added at this point and oxidation products were analyzed on a Hewlett-Packard 5880A chromatograph with a flame-ionization detector and capillary OV-5 (60 m × 0.20 mm) column. The H_2O_2 concentrations in catalytic solutions before and after the experiment were determined by iodometric titration and yields of oxidation products were calculated per mole of H_2O_2 consumed. Blank control experiments in the absence of catalyst(s) resulted in no detectable oxidation under the conditions used. All reactions were run at least in triplicate, and the data reported below are the average of these reactions. In the one-pot experiments, samples of the catalytic solution were withdrawn during the development of the reaction, while in the syringe–pump experiments only the final product mix was analysed.

Results and discussion

Ligand synthesis

The new ligand, 2,6-bis{3-[*N*,*N*-di(2-pyridylmethyl) amino]propoxy}benzoic acid (LH), containing a potentially bridging carboxylate moiety which is a part of the spacer that links two dipicolylamine groups has been prepared in a three-step synthesis with a general overall yield of *ca.* 60% (Scheme 1).

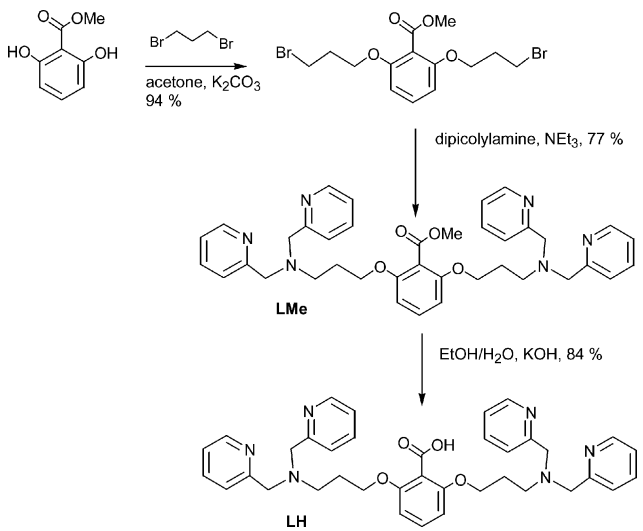

Scheme 1

The ligand was designed on the basis of relative ease of synthesis and potential fit to a dinuclear oxo-bridged metal (iron) core as determined by molecular modeling. The products LMe and LH have been identified by ^{1}H NMR spectroscopy, microanalysis, and, in the case of LMe, FAB mass spectrometry. The ^{1}H NMR spectra of LMe and LH are identical except for the methyl resonance at δ 3.61 that is present in the spectrum of LMe (the carboxylate proton of LH could not be detected due to broadening by exchange).

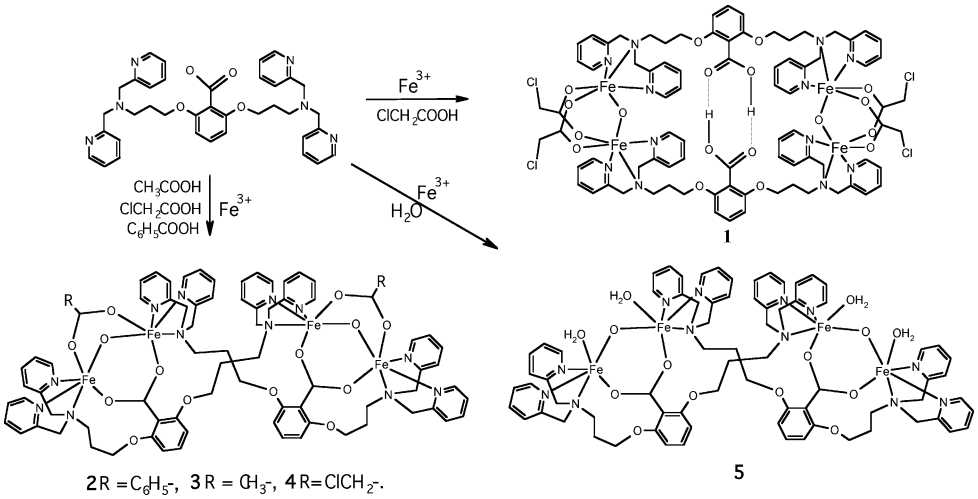

Scheme 2

Synthesis of complexes

Reactions of LH with an iron(III) salt followed by addition of a carboxylate salt leads to the formation of two kinds of tetranuclear complexes, depending on the nature of the added carboxylate (Scheme 2). Both types of tetranuclear complexes consist of linked $Fe^{III}_2(\mu\text{-}O)$ dimers, but the nature of the linkage between the dimers, and hence the structures of the complexes, differ.

Reaction of a seven-fold excess of chloroacetic acid with iron(III) perchlorate followed by addition of L to the mixture led to the formation of complex **1**, which was identified as $[Fe_4O_2(HL)_2(\mu\text{-}O_2CCH_2Cl)_4](ClO_4)_4$ on the basis of mass spectrometry. It was possible to grow crystals of **1** from a MeOH/MeCN solution and its crystal structure was determined in order to confirm the proposed tetranuclear structure. Complexes **2**, **3** and **4** were prepared by addition of benzoate, acetate or chloroacetate anions to the reaction mixture. The stoichiometric formulas of these complexes were established on the basis of their mass spectra, and these formulas indicate that **2–4** possess two less "non-ligand" carboxylates than **1**. However, the UV-Vis spectra of **2–4** (*vide infra*) suggest that the complexes contain Fe_2O clusters with irons bridged by two carboxylate moieties. One of these must be the deprotonated carboxylate associated with the framework ligand (L) and the determination of the crystal structure of **2** (*vide infra*) confirms this feature. Finally, reaction of LH with two equivalents of $Fe(ClO_4)_3$ in methanol leads to the formation of a green–brown product which has been assigned the formula $[Fe_2OL(H_2O)_2](ClO_4)_3$ **5** on the basis of UV-Vis, IR, and ^1H NMR spectroscopy.

Structural features of complexes 1 and 2. The cationic product of the reaction with chloroacetic acid, described above, consists of two Fe_2O dimers linked by protonated LH ligands to give the helical structure shown in Fig. 1. Selected bond lengths and angles are listed in Table 2. At the center of the "dimer of dimers" the carboxylic regions of the two LH ligands are hydrogen bonded in the head-to-head structure found commonly for crystallized carboxylic acids in the solid state. This interaction is shown in Fig. 2 with hydrogen atoms placed in idealized positions. The asymmetric region of the centrosymmetric triclinic unit cell consists of a complete cation with no imposed symmetry. Within the independent μ-oxodiiron units, iron atoms are bridged by two chloroacetate ligands while the non-bridging facial positions are filled by two di(picolyl)amine moieties from two molecules of LH, so that the two LH ligands link the adjacent μ-oxodiiron units. Sessler and coworkers found a similar extended bridge linking two Fe_2O units for the $[Fe_2L^2(\mu\text{-}O)(\mu\text{-}HCO_2)_2(HCO_2)_2]_2$ dimer, where L^2 = 1,3-bis((bis(1-methylimidazol-2-yl)phenylmethoxy)methyl)-benzene.[17] Within complex **1** the average Fe-μ-oxo distance is 1.79 Å and the average Fe–O–Fe angle is 121.8°; the intra-dimer Fe–Fe distances are 3.102(4) Å [Fe(1)–Fe(2)] and 3.138(4) Å [Fe(3)–Fe(4)] while the interdimer Fe–Fe distances vary from *ca.* 10.5 Å to 10.8 Å. The conformation of the linking ligands is such that the whole molecule acquires a helical shape, with a dihedral angle between the Fe–O–Fe planes in **1** of 42.5°. Detailed features within the inner coordination spheres of the four iron atoms are similar and compare well with the metrical dimensions of other $[L_2Fe_2O(carboxylate)_2]^{+n}$ cations.[17–19] Iron lengths to the picolyl nitrogen *trans* to the Fe–oxo bond are roughly equal to the lengths to the tertiary amine nitrogens as a result of the *trans* influence of the strong Fe–oxo bond.

Structural characterization on complex **2** has shown that the composition and structure of the complex cation are fundamentally different from that of **1**. A view of the $[\{Fe_2(\mu\text{-}O)(L)(\mu\text{-}O_2CC_6H_5)\}_2]^{4+}$ cation is shown in Fig. 3 and selected bond lengths

Table 2 Selected bond lengths (Å) and angles (°) for the $[\{Fe_2O(LH)(ClCH_2CO_2)_2\}_2]^{4+}$ cation in complex **1**

Fe1–O1	1.776(6)	Fe3–O2	1.794(6)
Fe1–N1	2.196(8)	Fe3–N4	2.216(8)
Fe1–N2	2.215(9)	Fe3–N5	2.198(10)
Fe1–N3	2.100(10)	Fe3–N6	2.152(9)
Fe1–O3	2.028(8)	Fe3–O7	2.020(8)
Fe1–O5	2.013(7)	Fe3–O9	2.054(7)
Fe2–O1	1.787(6)	Fe4–O2	1.786(6)
Fe2–N7	2.209(9)	Fe4–N10	2.226(8)
Fe2–N8	2.140(8)	Fe4–N11	2.216(9)
Fe2–N9	2.220(10)	Fe4–N12	2.104(10)
Fe2–O4	2.023(9)	Fe4–O8	2.051(8)
Fe2–O6	2.036(7)	Fe4–O10	2.013(7)
Fe1–Fe2	3.102(4)	Fe1–O1–Fe2	121.1(4)
Fe3–Fe4	3.138(4)	Fe3–O2–Fe4	122.5(4)

Table 3 Selected bond lengths (Å) and angles (°) for the $[\{Fe_2O(L)(PhCO_2)_2\}_2]^{4+}$ cation in complex **2**

Fe1–O1	1.801(6)	Fe2–O1	1.774(6)
Fe1–N1	2.162(9)	Fe2–N4	2.252(8)
Fe1–N2	2.138(11)	Fe2–N5	2.195(9)
Fe1–N3	2.144(8)	Fe2–N6	2.209(11)
Fe1–O2	1.979(7)	Fe2–O3	2.037(7)
Fe1–O4	2.025(8)	Fe2–O5	2.048(7)
C1–O2	1.302(12)	C8—O4	1.279(11)
C1–O3	1.203(11)	C8–O5	1.279(10)
Fe1–Fe2	3.111(4)	Fe1–O1–Fe2	121.0(4)

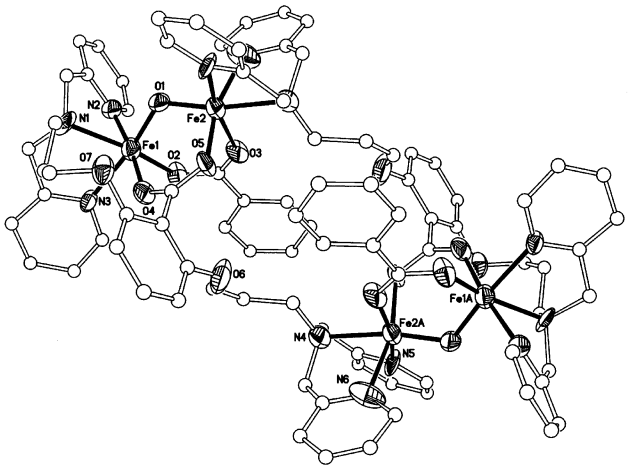

Fig. 3 An ORTEP drawing of the molecular structure of the $[\{Fe_2(\mu\text{-}O)(L)(\mu\text{-}O_2CC_6H_5)\}_2]^{4+}$ cation **2**. Each Fe_2O unit of the centrosymmetric cation is bridged by carboxylate groups from one L and from an exogenous benzoate anion. Thermal ellipsoids are drawn at the 30% level.

and angles are listed in Table 3. The cation is located about a center of inversion symmetry relating the two Fe_2O regions. As in the cation of **1**, the two Fe_2O units are linked by bridging L (LH) ligands. However, the carboxylic acid moieties of these ligands are deprotonated and bridge Fe_2O units to give a structure that is somewhat more strained than the open structure of **1**. Carboxylate groups of the benzoate ligands complete the bridged structure of the $[Fe_2O(carboxylate)_2]^{2+}$ regions of the dimer. Detailed features of the two Fe atoms of the crystallographically independent Fe_2O unit are significantly different (Table 3). The oxo bridge is unsymmetrical with the shorter Fe–O length to Fe2 (1.774(6) Å). The *trans* influence of this bond results in a rather long bond length to amine nitrogen N4 (2.252(8) Å), and generally longer bond lengths to all other atoms within the inner coordination sphere of Fe2, relative to equivalent lengths to Fe1. As a consequence of the different electronic properties of the two metals, the double bond of the benzoate carboxylate group is localized at C1–O3 (1.208(11) Å), with a significantly longer Fe2–O3 length (2.036(7) Å) relative to the long C1–O2 (1.297(12) Å) bond and shorter Fe1–O2 length (1.983(7) Å). This relatively subtle feature is significant in the carboxylate detachment mechanism for peroxide coordination in catalytic alkane oxidation reactions (*vide infra*). Other carboxylate groups of both structures have equivalent C–O lengths. This dissimilarity between the Fe centers results from the disposition of the di(picolyl)amine groups of L, folded on one side to coordinate with Fe1 at the dimer including the bridging carboxylate, and extended to bridge to the outer Fe_2O unit at Fe2 (Fig. 3).

Spectroscopic properties

Spectroscopic analyses indicate that the Fe_2O environments in **3**, **4** and **5** are similar to those found in **2**, and the spectroscopic properties are entirely consistent with those observed for (μ-oxo)bis(μ-carboxylato)diiron centers of other complexes.[1,19] Characteristic spectral features include high intensity of d–d transitions, low-energy shifts in charge-transfer absorptions compared with high-spin mononuclear iron complexes, and significant quadrupole splitting in the Mössbauer spectra. These unique features result from the considerable strength and, hence, the unusually short length, of the highly covalent Fe–oxo bond in these centers. The rather strong antiferromagnetic interaction ($-J = 100$–130 cm^{-1}) between the high-spin iron ions in such complexes is a consequence of significant overlap of partially occupied iron d orbitals with occupied p and s orbitals of the bridging oxygen. This interaction results in an increase in the intensity of d–d transitions. Because orbital overlap depends on the Fe–O distance and the Fe–O–Fe bond angle, the spectroscopic and magnetic characteristics of Fe_2O complexes are also correlated with these structural parameters.

The positions of the absorption maxima in the UV-Vis spectra and molar absorption coefficients of complexes **1–5** are listed in Table 4. The electronic spectra of Fe_2O complexes are usually subdivided into three regions.[1b] Region 1 (300–400 nm) contains two intense (ε/Fe = 3–6 × 10^3 M^{-1} cm^{-1}) absorptions due to LMCT transitions from the bridging oxo ligand to Fe(III) which are not always clearly resolved. Region 2 (400–550 nm) contains two or three absorptions whose intensities are lower than those of absorptions in region 1 by a factor of 5–10. These absorptions correspond to ligand field (LF) transitions enhanced by mixing with LMCT transitions from region 1. Region 3 (550–800 nm) contains a characteristically wide low-intensity LF ($^6A_1 \rightarrow {}^4T_2$)/LMCT band whose position is very sensitive to the Fe–O–Fe bond angle.[1] The Fe–O–Fe angle in **2** is ~121.0(4)°, and the proximity of the wide absorptions at 724 nm observed for **2** to analogous absorptions in **3–5** suggests that similar angles apply to the Fe_2O units in the latter complexes.

The vibrational characteristics of the Fe–O–Fe units in **1–5** were studied by IR spectroscopy. The ν_s(Fe–O–Fe) absorptions were observed at 530–540 cm^{-1} while the ν_{as} absorptions are obscured by other ligand absorptions in this region. Comparison of the IR spectra of complexes **1–5** (*cf.* Table 4) and $[\{Fe_2O(dpab)\}_2](ClO_4)_8$,[20] in which the same terminal dipicolylamine ligands are present but carboxylate bridges are absent, suggests that the strong absorptions of approximately equal intensity in the IR spectra of complexes **1–5** can be identified as the absorptions corresponding to asymmetric and symmetric vibrations of both carboxylates. The $\Delta\nu$ value, which characterizes the difference in the positions of these absorptions, provides support for bridging bidentate coordination of both carboxylates in complexes **1–5** (Table 4); this value is consistent with the range $\Delta\nu = 110$–170 cm^{-1}, which is typical of bridging carboxylate groups in diiron complexes of this type.

Mössbauer ΔE_Q values of ~1.6 mm s^{-1} are found for short Fe–O bonds in doubly or triply bridged Fe_2O clusters, whereas significantly lower quadrupole splitting is indicative of the elongation of this bond in mononuclear, hydroxo-bridged, or trinuclear (or polynuclear) iron complexes. The spectrum of complex **2** (Fig. 4) with the parameters $\delta = 0.49$, $\Delta E_{Q1} = 1.47$, and $\Delta E_{Q2} = 1.82$ mm s^{-1}, is similar to the spectrum of complex **5**

Table 4 Spectroscopic and geometric properties of the dinuclear complexes $[Fe_4O_2(L)_2(\mu\text{-}O_2CCH_2Cl)_4](ClO_4)_4$ **1**, $[\{Fe_2(\mu\text{-}O)(L)(\mu\text{-}O_2CC_6H_5)\}_2](ClO_4)_4$ **2**, $[\{Fe_2(\mu\text{-}O)(L)(\mu\text{-}O_2CCH_3)\}_2](ClO_4)_4$ **3**, $[\{Fe_2(\mu\text{-}O)(L)(\mu\text{-}O_2CCH_2Cl)\}_2](ClO_4)_4$ **4**, $[Fe_2O(L)(H_2O)_2](ClO_4)_3$ **5**, and the azido derivative of met-hemerythrin ($metN_3Hr$)

		1	**2**	**3**	**4**	**5**	$metN_3Hr$
λ_{max}/nm (ε/M^{-1} cm^{-1})	LMCT	344 (17000)	340 (17600)	344 (12400)	344 (19100)	330 (4000)	326 (3375)
	LMCT	380 (12400)					380 (2150)
	$^6A_1 \rightarrow {}^4T_2$	472 (3380)	467 (2650)	467 (2650)	472 (3200)	474 (649)	446 (1850)
	$O^{2-} \rightarrow$ Fe *CT*	510 (2650)	510 (1820)	505 (2100)	505 (2200)	505 (590)	497 (325)
	$^6A_1 \rightarrow {}^4A_1, {}^4E$	555 (sh)	550 (sh)	550 (sh)	550 (sh)	555 (sh)	530 (sh)
	$^6A_1 \rightarrow {}^4T_2$/LMCT	721 (622)	725 (450)	723 (700)	725 (470)	724 (97)	680 (95)
ν_s(Fe–O–Fe)/cm^{-1}		537	539	535	530	537	507
$\Delta\nu$(COO)/cm^{-1}		152	134	108	163	122	
δ/mm s^{-1}			0.49;0.48			0.49;0.45	0.50
ΔE_Q/mm s^{-1}			1.47;1.82			1.68;0.95	1.90
Fe–Fe/Å		3.102(4); 3.138(4)	3.111(4)				3.23
Fe–O–Fe/°		121.1(4); 122.5(4)	121.0(4)				130

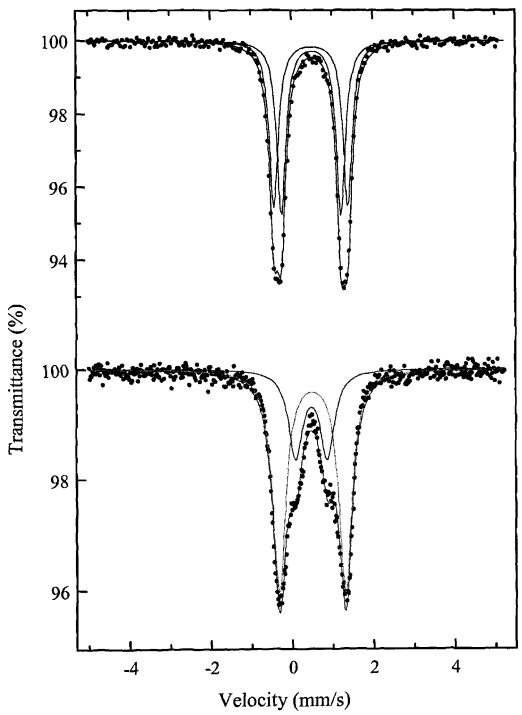

Fig. 4 Mössbauer spectra recorded on $[\{Fe_2(\mu\text{-}O)(L)(\mu\text{-}O_2CC_6H_5)\}_2](ClO_4)_4$ **2** (top) and $[Fe_2O(L)(H_2O)_2](ClO_4)_3$ **5**; see text for experimental details.

($\Delta E_Q = 1.68$ mm s^{-1}) and spectra that are characteristic of structures in which two high-spin Fe(III) ions are antiferromagnetically coupled in the $Fe_2O(\mu\text{-}RCO_2)_2$ system. The inequivalence of iron atoms in **2** is detected in the Mössbauer spectrum by the presence of two overlapping quadrupole doublets in a 1 : 1 ratio. The large $\Delta E_{Q2} = 1.82$ mm s^{-1} suggests a significant distortion from octahedral symmetry for one of the iron centers as noted in the X-ray structure of **2** (*vide supra*). The superposition of two overlapping quadrupole doublets with equal intensity leads to broadening of the Mössbauer spectra for all of the complexes (**1–5**, average $\Delta E_Q \sim 1.65$) in agreement with their tetranuclear structures. The appearance of an additional component with $\Delta E_Q < 1$ in the Mössbauer spectrum of complex **5** is probably due to the admixture of an $Fe(OH)_2Fe$ complex.

Table 5 ^{1}H NMR data for the complexes of LH/L and the structurally similar $[Fe_2O((PyCH_2)_2NCH_2CO_2)_2(BzO)]^{3+}$ (**a**);[19] see ESI† for NMR spectra

H	**1**	**2**	**3**	**4**	**5**	**a**
o-Py	28	28.4	27.5	29	26	24
N-CH_2-Py	15.6	15.49	15.47	15.7	15.4 14.0	16.2
m-Py	12.0	12.14 11.62	12.06	12.0	11.6 11.3	12.4
OAc	11.5		11.56[a]	11.6		
m-Ph	8.5	8.5	8.49	8.5	8.9 8.6	8.5
p-Ph	7.8	7.9	7.7	7.76	8.0	6.8
p-Py	7.4	7.7	7.2		7.3	6.7

[a] The signal disappears when acetate is replaced with deuteroacetate.

The weak paramagnetism of the Fe_2O complexes, resulting from strong antiferromagnetic coupling between the Fe(III) atoms, leads to relatively well-resolved signals in their ^{1}H NMR spectra and narrow spectral widths (up to 40 ppm). Assignments of the ^{1}H NMR spectra of the complexes in this study are based on their similarities to the spectra of oxo-bridged diiron complexes of related ligands, *viz.* $\{PyCH_2\}_2N(CH_2)_nCO_2^-$ (n = 1,2).[19] The signals in the ^{1}H NMR spectra of complexes **1–5** (Table 5) are all located in the region 0–28 ppm, suggesting similar J values (and Fe_2O (sub)structures) for all complexes. There are broad features above δ 20 ($PyCH_2$ and *o*-Py protons), sharper signals at δ 15–18 (*m*-Py protons), and a very sharp signal at δ *ca.* 6 (*p*-Py protons). In addition, there are sharp signals from the polymethylene chain of L at δ 3–9. The paramagnetically shifted and broadened signals due to the terminally coordinated $(PyCH_2)_2N$ group in **1–5** (see Fig. S1, ESI†) are very similar to the signal pattern observed for the complex $[Fe_2O((PyCH_2)_2NCH_2CO_2)_2(BzO)]^{3+}$, which contains a similar di(picolyl)amine ligand moiety.[19] This fact suggests that there is some structural similarity between **1–5** and $[Fe_2O((PyCH_2)_2NCH_2CO_2)_2(BzO)]^{3+}$.

Electrospray (ES) ionization mass spectrometry

The mass spectra of CH_3CN solutions of **1–5** were measured on a prototype time-of flight mass spectrometer equipped with an ion source with ES ionization. Attempts to detect the molecular ion of **1** were unsuccessful but prominent ions were detected at m/z 952, 601 and 426; these ions are consistent with the molecular formulation(s) $\{[Fe_4L_2(ClCH_2CO_2)_2](ClO_4)_{4-x}\}^{x+}$ (x = 2–4,

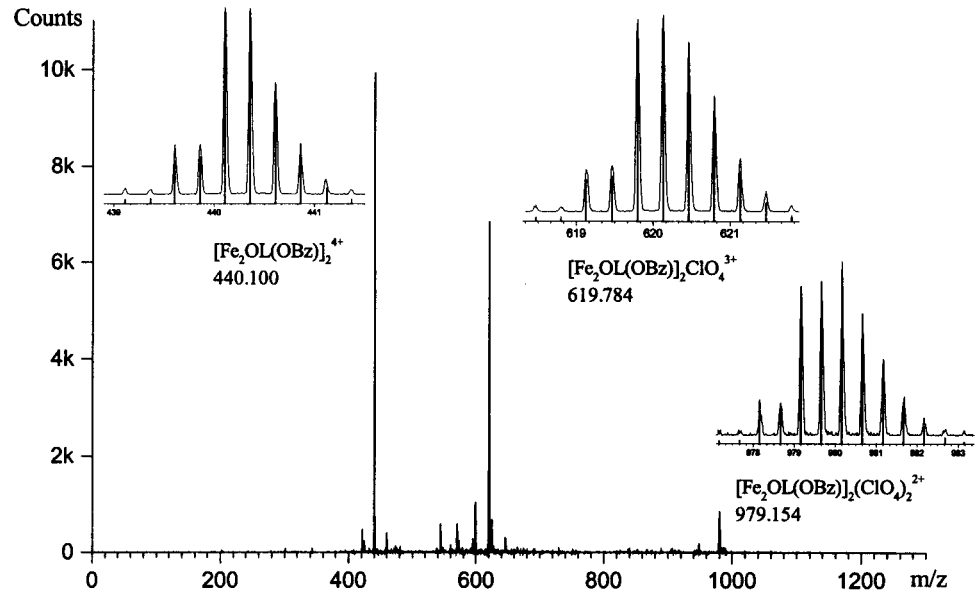

Fig. 5 An electrospray (ES) ionization mass spectrum of $[\{Fe_2(\mu\text{-}O)(L)(\mu\text{-}O_2CC_6H_5)\}_2]^{4+}$ **2** in acetonitrile. Inserts show the fine structure of the molecular ion signals and the theoretical isotope distributions.

respectively), corresponding to complex **4** (*vide infra*). We have found that complex **4**, $[Fe_4O_2(L)_2(\mu\text{-}O_2CCH_2Cl)_2](ClO_4)_4$, is in equilibrium with complex **1**, $[Fe_4O_2(LH)_2(\mu\text{-}O_2CCH_2Cl)_4](ClO_4)_4$, in solution, but that the equilibrium can be shifted towards the formation of **1** by addition of a relatively large excess of a carboxylic acid. The mass spectrum suggests that **1** readily loses two chloroacetic acid molecules in the gas phase.

At a concentration of 3×10^{-4} M of complex **2**, the mass spectrum (Fig. 5) exhibits three ions of *m*/*z* 440, 619 and 979, which correspond to $[Fe_2OL(OBz)]_2^{4+}$, $\{[Fe_2OL(OBz)]_2(ClO_4)\}^{3+}$ and $\{[Fe_2OL(OBz)]_2(ClO_4)_2\}^{2+}$. Similarly, complex **3** gives ions at *m*/*z*: 409, 578 and 917 corresponding to $[Fe_2OL(OAc)]_2^{4+}$, $\{[Fe_2OL(OAc)]_2(ClO_4)\}^{3+}$ and $\{[Fe_2OL(OAc)]_2(ClO_4)_2\}^{2+}$. The mass spectrum of **4** was found to be identical to that of **1** (*vide supra*) and in full agreement with the proposed formula for **4**. On the other hand, complex **5** appears to fragment even under electrospray ionization conditions, and no ions attributable to the complex could be detected.

Electrochemical properties

For complexes **2** and **5**, two irreversible two-electron reduction waves could be detected, the potentials of which are listed in Table 6. A quantitative estimate of the number of electrons transferred was achieved by comparing the height of reduction peak currents to that of the first (one-electron) reduction of the trinuclear complex $[(MeOH)(H_2O)_2Fe_3(\mu_3\text{-}O)(PBAH^+)_6]^{7+}$ (PBA = 2-(pyrid-2-ylmethoxy)benzoate) under the same experimental conditions of concentration and scan rate.[10] This complex was chosen as a standard because of its comparable size, and, hence, close value of diffusion coefficient, to **2** and **5**. For complex **3** only one irreversible reduction wave is seen at –0.41 V (*vs* SCE, not listed in Table 6). A similar instability with respect to electrochemical reduction has been observed for $[Fe_2O(MeCO_2)_2(HBpz_3)_2]$, for which an irreversible reduction occurs at –0.76 V (*vs*. SCE),[18b]

Table 6 Potentials of peaks of reduction of complexes **2** and **5** ($C = 1 \times 10^{-3}$ M) in MeCN/0.1 M Bu_4NPF6 on a glassy carbon electrode ($v = 0.2$ V s^{-1}) at +15 °C. Numbers of transferred electrons are specified in brackets.

Complex	E_p/V (SCE)	
2	–0.39 (2e)	–1.75 (2e)
5	–0.28 (2e)	–1.48 (2e)

as well as several other complexes.[1b] The values of E_p obtained in these experiments are in agreement with the observation that reduction potentials of Fe_2O complexes depend on the basicity and charge of the bridging anionic ligand.[21]

As the electrochemically active binuclear moieties in the tetranuclear complex are separated by relatively large distances (~10 Å) and show no evidence for interdimer electronic coupling, they are reduced to isolated binuclear entities at identical potentials and undergo two synchronous one-electron transfers. Thus, the investigated complexes are reduced from the $\{Fe(III)Fe(III)\}_2$ oxidation state to the fully reduced $\{Fe(II)Fe(II)\}_2$ oxidation state in two two-electron ($1\ e^- + 1\ e^-$) reductions. For comparison, the tetranuclear complex $[LFe_2OA]_2(PF_6)_4$, (A = the dianion of glutaric acid), shows two analogous consecutive peaks at −0.500 and 0.635 V (*vs*. $Ag/AgNO_3$).[22]

The electrochemical behavior of **2** and **5** suggests the possibility of preparing mixed valence analogues of these complexes. The difference between the first and second reduction potentials for complexes **2** (1.36 V) and **5** (1.20 V) specifies the thermodynamic stability of their mixed valence states. As to kinetic stability, the irreversible character of the peaks (which remains even at −30 °C) indicates that the mixed valence (Fe(III)Fe(II)) and fully reduced all-ferrous forms of the complexes are unstable on the timescale of cyclic voltammetry, and/or that a specific stage of the electron transfer process is slow due to structural reorganization induced by the transfer of an electron. It is likely that such structural

reorganization only consists of relatively minor changes in the coordination spheres of the irons and not a change in the nuclearity of the complex, at least in the case of electrochemically generated mixed valence species. If the tetranuclear composition of complexes **2** and **5** was not retained and the complexes were to fragment upon reduction, then a substantially larger current should be observed for the second reduction wave because diffusion of mononuclear complexes should be much higher than for di- or tetranuclear complexes. As expected, the addition of benzoate to a solution of complex **5** resulted in a negative shift in reduction potential, in agreement with the formation of cation **2** (Table 6).

Catalytic activity of complexes 2, 3 and 5 in alkane oxidation with hydrogen peroxide

An acetonitrile solution containing one of the iron complexes (**2**, **3** or **5**; 0.70 mM), hydrogen peroxide and cyclohexane, in a molar ratio of 1 : 420 : 1000, was stirred for 2.5 h at room temperature in air. Cyclohexanol and cyclohexanone were observed to form at a turnover range of 4 to 7 (Table 7). Complex **1** is not active under these conditions and complex **4** was not checked. The yield per H_2O_2 consumed is not large (7–13%) due to disproportionation of H_2O_2 as a side reaction. It was possible to increase the conversion of oxidant into organic products when the oxidant was delivered by a syringe pump to suppress disproportionation.[23] This is especially the case for the aqua complex **5** (see Table 7), where the yield is increased substantially by the use of a syringe pump. The high stereospecificity in the oxidation of *cis*-1,2-dimethylcyclohexane points to a metal-based molecular mechanism[24] similar to the mechanism of oxo transfer suggested for enzymes such as cytochrome P-450[25] and sMMO.[26] Catalytic oxidation of cyclohexane by complex **2** was also performed under a vigorous argon purge in order to remove any traces of dioxygen and to check its influence on the observed results.[24b] In order to exclude a diminution of the concentration of the relatively volatile cyclohexane in the catalytic solution, the argon gas was saturated with cyclohexane vapors. No differences could be detected between the experiments carried out under argon or air, indicating that there is no involvement of O_2 in this oxidation.

The catalytic activity of complexes **2** and **3** is lower than that of the more short lived complex **5** (see Table 7). The most plausible mechanism for alkane oxidation requires initial coordination of H_2O_2 at one metal of the Fe_2O dimer. In cases where there is a dicarboxylate bridge between irons, this requires prior detachment of a carboxylate oxygen to create a vacant coordination site.[27] Structural features of the benzoate ligand of **2** show a localized C=O double bond for the carboxylate and lengths to the metals that suggest that it is poised for detachment from Fe2 to create a site for H_2O_2 addition. However, during the catalytic cycle there is constant competition between the detached carboxylate oxygen and peroxide for the vacant coordination site. Complete dissociation of the carboxylate appears unlikely since the activity of the complex remains less than that of **5**, and there is a correlation between catalytic activity and redox potential (Table 6). Further, the activity of **5** is expected to be higher since it contains twice the number of labile coordination sites than the carboxylate-detached Fe_2O dimer. The high stereospecificity observed for all three complexes is a clear indication that the oxidation reaction occurs at one (or both) of the iron centers, and, to our knowledge, these are the first observations of *stereospecific* alkane oxidation catalyzed by (μ-carboxo)diiron complexes.

In general, stereospecific alkane oxidation reactions catalyzed by non-heme iron complexes are rare,[12] and every new example is interesting. The ligand composition of iron in complexes **2**, **3** and **5** is similar to that in the iron tripicolylamine (TPA) complexes[29] that also catalyze stereospecific alkane oxidation. The ligand environments in **2**, **3**, and **5** differ from the TPA complexes in the respect that one pyridine nitrogen (from the TPA ligand) has been replaced by an oxygen of a carboxylate. In comparison with Fe–TPA complexes, the rate of oxidation by complexes **2**, **3** and **5** is slower, perhaps due to a geometric constraint created by the framework of ligand L. At the same time these complexes are stable at high H_2O_2 concentration allowing them to be used in "one-pot" experiments. It has been shown in earlier papers[28,29] that mononuclear iron(II) complexes used in such reactions are transformed into dinuclear Fe_2O complexes a short time after the beginning of the reaction. However, the data in these papers does not point uniquely to either a mono- or dinuclear complex as the active catalyst in oxo transfer and usually a mechanism involving a mononuclear center is suggested.[29] According to mass spectrometry data, the dinuclear structure of complex **2** is stable up to micromolar concentrations in MeCN due to the encapsulation of the iron ions by the framework polydentate ligand. Therefore

Table 7 Alkane oxidation with H_2O_2 catalyzed by iron complexes[a]

	Cyclohexane, one-pot			Cyclohexane, syringe pump				
Complex	TN	A/K	*Y* (%)	TN	A/K	*Y* (%)	*cis*-DMCH RC (%)	Ref.
$[Fe_2O(phenNO_2)_4(H_2O)_2](ClO_4)_4$	14.0	2.5	10				72[b] 82[c]	19
$[Fe^{II}(tpa)(MeCN)_2](ClO_4)_2$				3.0	5.0	32	100	23
5	6.5	2.4	13	4.3	3.7	52	94	This work
2	4.5	2.3	9	3.6	2.3	13	93	This work
3	4.0	2.5	6.5	3.5	3.0	12	93	This work

[a] Introduction of H_2O_2: "one-pot"—as one portion at the beginning of the reaction together with other reagents, "syringe pump"—delivered dropwise by syringe pump over the time of the reaction. TN—Average turnover number, mole of products (A + K)/mole of catalyst, A—cyclohexanol, K—cyclohexanone, Y —yield of products (A + K) per H_2O_2 consumed, *cis*-DMCH—*cis*-1,2-dimethylcyclohexane, RC—retention of configuration in the oxidation of the tertiary C–H bonds of *cis*-DMCH, expressed as the ratio of the corresponding tertiary alcohols: (*cis* − *trans*)/(*cis* + *trans*). [b] Value obtained for the oxidation of *trans*-1,4-dimethylcyclohexane. [c] E. A. Gutkina, O. N. Gritsenko, unpublished data.

it is possible to conclude in our case that the Fe_2O centers with labile coordination sites are active in oxo-transfer catalysis.

The framework octadentate ligand, 2,6-bis{3-[*N*,*N*-di(2-pyridylmethyl)-amino]propoxy}benzoic acid (LH) prepared in this project forms tetranuclear iron complexes **1–5** in which separated Fe_2O cores are linked *via* two molecules of LH or its corresponding anion L. The structural and spectroscopic results obtained provide evidence for the "dimer of dimers" structure of complexes **2–5**. When the carboxylate group of L bridges iron ions inside the Fe_2O core, the resulting complexes (**2**, **3** and **5**) are active in the catalysis of stereospecific alkane oxidation by hydrogen peroxide, thus mimicking the corresponding diiron centres of the MMO enzymes. These complexes provide new insights for further structural development of chemical models for MMO.

Acknowledgements

This work was supported by the Russian Foundation for Basic Research (project no. 97-03-32253 and 00-15-97367), the Swedish Research Council (VR), the Royal Swedish Academy of Sciences, CRDF (grant # RC1-2058) and INTAS (grant # 97–1289). We thank Prof. A. F. Dodonov, Dr V. I. Kozlovski and I. V. Soulimenkov, Institute of Energetic Problems of Chemical Physics, Chernogolovka, Russia and Dr Kenneth B. Jensen, Department of Chemistry, Odense University, Denmark for electrospray mass spectrometry of the iron complexes. We are also grateful to Dr N. S. Ovanesyan for Mössbauer spectroscopy measurements, Prof. Åke Oskarsson for assistance with X-ray data collection and Prof. Bernt Krebs for useful discussions.

References

1 (*a*) E. Y. Tshuva and S. J. Lippard, *Chem. Rev.*, 2004, **104**, 987; (*b*) D. Kurtz, M., *Chem. Rev.*, 1990, **90**, 585.
2 S. Ménage, E. C. Wilkinson, L. Que, Jr. and M. Fontecave, *Angew. Chem., Int. Ed. Engl.*, 1995, **34**, 203.
3 L. Berchet, M. N. Collomb-Dunand-Sauthier, P. Dubordeaux, W. Moneta, A. Deronzier and J.-M. Latour, *Inorg. Chim. Acta*, 1998, **282**, 243–246.
4 D. E. Fenton and H. Okawa, *Chem. Ber./Recl. Trav. Chim. Pays-Bas*, 1997, **130**, 433–442.
5 D. M. Kurtz, Jr., *J. Biol. Inorg. Chem.*, 1997, **2**, 159–167.
6 B. J. Wallar and J. D. Lipscomb, *Chem. Rev.*, 1996, **96**, 2625–2657.
7 C. Hemmert, M. Verelst and J.-P. Tuchagues, *Chem. Commun.*, 1996, 617–618.
8 V. M. Trukhan and A. A. Shteinman, *Russ. Chem. Bull., Int. Ed.*, 1997, **46**, 202–203.
9 A. Hazell, K. B. Jensen, C. J. McKenzie and H. Toftlund, *J. Chem. Soc., Dalton Trans.*, 1993, 3249–3255.
10 V. M. Trukhan, I. L. Eremenko, N. S. Ovanesyan, A. A. Pasynskii, I. A. Petrunenko, V. V. Strelets and A. A. Shteinman, *Russ. Chem. Bull., Int. Ed.*, 1996, **45**, 1981–1987.
11 M. Costas, M. H. Mehn, M. P. Jensen and L. Que, Jr., *Chem. Rev.*, 2004, **104**, 939–986.
12 (*a*) A. A. Shteinman, *Russ. Chem. Bull., Int. Ed.*, 2001, **50**, 1795–1810; (*b*) M. Costas, K. Chen and L. Que, Jr., *Coord. Chem. Rev.*, 2000, **200–202**, 517–544; (*c*) Y. Mekmouche, S. Menage, C. Toia-Duboc, M. Fontecave, J.-P. Galey, C. Lebrun and J. Pecaut, *Angew. Chem., Int. Ed.*, 2001, **40**, 949–952.
13 (*a*) M. S. Seo, J.-H. In, S. O. Kim, N. Y. Oh, J. Hong, J. Kim, L. Que, Jr. and W. Nam, *Angew. Chem., Int. Ed.*, 2004, **43**, 2417–2420; (*b*) F. Avenier, L. Dubois and J.-M. Latour, *New J. Chem.*, 2004, **28**, 782–784.
14 V. M. Trukhan, C. G. Pierpont, K. B. Jensen, E. Nordlander and A. A. Shteinman, *Chem. Commun.*, 1999, 1193–1194.
15 E. Lambert, B. Chabut, S. Chardon-Noblat, A. Deronzier, A. Bousseksou, J.-P. Tuchagues, G. Chottard, M. Bardet and J.-M. Latour, *J. Am. Chem. Soc.*, 1997, **119**, 9294–9437.
16 O. A. Mirgorodskaya, A. A. Shevchenko and A. F. Dodonov, *Anal. Chem.*, 1994, **66**, 99–107.
17 J. L. Sessler, J. D. Hugdahl, V. Lynch and B. Davis, *Inorg. Chem.*, 1991, **30**, 334–336.
18 (*a*) K. Wieghardt, K. Pohl and W. Gebert, *Angew. Chem., Int. Ed. Engl.*, 1983, **22**, 727–729; (*b*) W. H. Armstrong, A. Spool, G. C. Papaefthymiou, R. B. Frankel and S. J. Lippard, *J. Am. Chem. Soc.*, 1984, **106**, 3653–3667; (*c*) H. Toftlund, K. S. Murray, P. R. Zwack, L. F. Taylor and O. P. Anderson, *J. Chem. Soc., Chem. Commun.*, 1986, 191–192; (*d*) J. R. Hartman, R. L. Rardin, P. Chaudhuri, K. Pohl, K. Wieghardt, B. Nuber, J. Weiss, G. C. Papaefthymiou, R. B. Frankel and S. J. Lippard, *J. Am. Chem. Soc.*, 1987, **109**, 7387–7396; (*e*) J. B. Vincent, J. C. Huffman, G. Christou, Q. L. Li, M. A. Nanny, D. N. Hendrickson, R. H. Fong and R. H. Fish, *J. Am. Chem. Soc.*, 1988, **110**, 6898–6900; (*f*) P. Gomez-Romero, N. Casari-Pastor, A. Ben-Hussein and G. B. Jameson, *J. Am. Chem. Soc.*, 1988, **110**, 1988–1900; (*g*) Y. Nishida, S. Haga and T. Tokii, *Chem. Lett.*, 1989, 109–111; (*h*) R. H. Beer, W. B. Tolman, S. G. Bott and S. J. Lippard, *Inorg. Chem.*, 1989, **28**, 4557–4559; (*i*) H. Adams, N. A. Bailey, J. D. Crane, D. E. Fenton, J.-M. Latour and J. M. Williams, *J. Chem. Soc., Dalton Trans.*, 1990, 1727–1733; (*j*) F.-J. Wu, D. M. Kurtz, K. S. Hagen, P. D. Nyman, P. C. Debrunner and V. A. Vankai, *Inorg. Chem.*, 1990, **29**, 5174–5183; (*k*) W. B. Tolman, S. Liu, J. G. Bentsen and S. J. Lippard, *J. Am. Chem. Soc.*, 1991, **113**, 152–164; (*l*) S. P. Watton, A. Masschelein, J. Rebek, Jr. and S. J. Lippard, *J. Am. Chem. Soc.*, 1994, **116**, 5196–5205; (*m*) U. Bossek, H. Hummel, T. Weyhermüller, E. Bill and K. Wieghardt, *Angew. Chem., Int. Ed. Engl.*, 1995, **34**, 2642–2645; (*n*) M. Kodera, H. Shimakoshi, M. Nishimura, H. Okawa, S. Ijima and K. Kano, *Inorg. Chem.*, 1996, **35**, 4967–4973; (*o*) S. C. Payne and K. S. Hagen, *J. Am. Chem. Soc.*, 2000, **122**, 6399–6405.
19 S. Ménage and L. Que, Jr., *New J. Chem.*, 1991, **15**, 431–438.
20 V. M. Trukhan, A. A. Shteinman, unpublished data, dpab = 1,3-di-((di-(2-pyridylmethyl)amino)propoxy)benzene.
21 (*a*) B. T. Weldon, D. E. Wheeler, J. P. Kirby and J. K. McCusker, *Inorg. Chem.*, 2001, **40**, 6802–6812; (*b*) R. C. Holz, T. E. Elgren, L. L. Pearce, J. H. Zhang, C. J. O'Connor and L. Que, Jr., *Inorg. Chem.*, 1993, **32**, 5844–5850.
22 J. L. Sessler, J. W. Sibert, V. Lynch, J. T. Markert and C. L. Wooten, *Inorg. Chem.*, 1993, **32**, 621–626.
23 J. Kim, R. G. Harrison, C. Kim and L. Que, Jr., *J. Am. Chem. Soc.*, 1996, **118**, 4373–4379.
24 (*a*) V. S. Kulikova, O. N. Gritsenko and A. A. Shteinman, *Mendeleev Commun.*, 1996, 119–121; (*b*) K. Chen and L. Que, Jr., *J. Am. Chem. Soc.*, 2001, **123**, 6327–6337.
25 P. R. Ortiz de Montellano, Ed. *Cytochrome P-450: Structure, Mechanism, and Biochemistry*, 2nd edn, Plenum, New York, 1995.
26 A. M. Valentine and S. J. Lippard, *J. Chem. Soc., Dalton Trans.*, 1997, 3925–3932.
27 (*a*) R. L. Rardin, W. B. Tolman and S. J. Lippard, *New J. Chem.*, 1991, **15**, 417–430; (*b*) R. F. Moreira, E. Y. Tshuva and S. J. Lippard, *Inorg. Chem.*, 2004, **43**, 4427–4434.
28 K. Chen and L. Que, Jr., *J. Am. Chem. Soc.*, 2001, **123**, 6327–6337.
29 E. A. Gutkina, T. B. Rubtsova and A. A. Shteinman, *Kinet. Katal.*, 2003, **44**, 116–121.